GIMC-based switching control of magnetically suspended steel plates

Proceedings of the 2006 IEEE
International Conference on Control Applications
Munich, Germany, October 4-6, 2006

GIMC-based Switching Control of Magnetically Suspended Steel Plates

Hideto Maruyama and Toru Namerikawa

Abstract— **This paper deals with robust control of magnetically suspended steel plates by using a switching control based on Generalized Internal Model Control (GIMC) structure. First, we derive a mathematical model for the magnetically suspended steel plate. The system is a multi-input and multi-output unstable mechatronic system. Then we design a robust controller which achieves both of high performance and high robustness for the magnetically suspended steel plates. GIMC structure is constructed with a general outer feedback loop and an inner loop. The outer-loop controller is a nominal high performance controller and it can be used for the nominal plant. On the other hand, the inner-loop controller is designed via the parameterization of a set of stabilizable controllers. Finally, several experimental results show that the GIMC structure based switching controller has both of high performance for the nominal plant and the high robustness for the perturbed plants compared with a μ controller.**

I. INTRODUCTION

The effectiveness of robust control design techniques such as $\mathscr{H}_\infty$ control, μ-synthesis has been shown via plenty of applications, but almost all robust control design techniques sacrifice nominal performance, because they are based on the worst possible scenarios which may occur in a only particular situation [1], [2]. Robust stability for the worst-case scenario is still important. Then a desired property for the control systems should achieve both of high nominal performance and high robust stability.

It is well-known that general control architecture cannot achieve both performance and robustness because there exist a tradeoff between these specifications. Then multiple control architectures should be used and they should be switched to adapt condition of the controlled plant. For this problem, "Generalized Internal Model Control structure" was proposed by Kemin Zhou [3], [4], where GIMC structure is one of generalized structure of IMC by introducing outer feedback controller. This structure can switch controllers according to a residual information between the plant and its internal model. This method had been applied to gyroscope and motor control and the effect for fault-tolerant property was confirmed[5], [6]. But it has not been applied to strictly unstable plants yet. An application of multiple free parameters was proposed[7], but this method has not been verified yet experimentally.

Hence, our goal is to apply the GIMC structure to a strictly unstable and MIMO magnetically suspended steel plate and evaluate its effectiveness via control experiments[8], [9]. The magnetically suspended steel plate is a four-input and four-output MIMO system and it is unstable and infinite dimensional system. Here, we consider the multiple suspended objects and verify that GIMC structure achieves both of high nominal performance and high robustness.

We design three robust controllers based on the $\mathscr{H}_\infty$ mixed sensitivity problem and they are appropriately switched in the GIMC structure according to the internal residual signal. For comparison, we also design a robust single controller which achieves robust performance condition based on the structured singular value μ.

We show that the conventional μ-controller has the robust performance but the nominal performance is sacrificed for improving robustness. On the other hand, the proposed GIMC controller has better nominal performance compared with the μ controller, and also achieves higher robust stability for multiple plants.

II. GIMC STRUCTURE

A. Definition and Basic Property

Let $P(s)$ be a nominal plant model of LTI plant $\tilde{P}(s)$ and $K_0(s)$ be a stabilizing controller for $P(s)$. Suppose that K_0 and P have the left coprime factorizations expressed by

$$P(s) = \tilde{M}(s)^{-1}\tilde{N}(s), \quad K_0(s) = \tilde{V}(s)^{-1}\tilde{U}(s) \tag{1}$$

It is well known that every stabilizing controller $K(s)$ for $P(s)$ can be written in (2) and (3) where $Q(s) \in RH_\infty$ is a free-parameter,

$$K(s) = (\tilde{V}(s) - Q(s)\tilde{N}(s))^{-1}(\tilde{U}(s) + Q(s)\tilde{M}(s)), \tag{2}$$

$$\det(\tilde{V}(\infty) - Q(\infty)\tilde{N}(\infty)) \neq 0. \tag{3}$$

A typical GIMC structure is shown in Fig.1. This has an outer feedback loop($K_0(s) = \tilde{V}(s)^{-1}\tilde{U}(s)$) and an internal feedback loop. This structure is similar to the well-known Internal Model Control, and is generalized by introducing a dynamic controller.

Note that the reference signal $ref(t)$ in Fig.1 enters into the stabilizing controller $K(s)$, but the transfer function from $y(t)$ to $u(t)$ is same with $K(s) = (\tilde{V}(s) - Q(s)\tilde{N}(s))^{-1}(\tilde{U}(s) + Q(s)\tilde{M}(s))$. Hence the stability of the system is same with $K(s)$. The free-parameter $Q(s) \in RH_\infty$ can be chosen to achieve (3) and $K(s)$ is a set of the stabilizing controllers.

GIMC structure can achieve both high performance and high robustness because it utilizes both $K_0(s)$ and $K(s)$ based on an internal residual signal $f(s)$. The residual signal $f(s)$ can be expressed in (4)[4].

$$f(s) = \tilde{N}(s)u(s) - \tilde{M}(s)y(s) \tag{4}$$

H. Maruyama is with Department of Mechanical Engineering, Nagaoka University of Technology, 1603-1 Kamitomioka, Nagaoka 940-2188 JAPAN.
T. Namerikawa is with Division of Electrical Engineering and Computer Science, Graduate School of Natural Science and Technology, Kanazawa University, Kakuma, Kanazawa 920-1192 JAPAN. toru@t.kanazawa-u.ac.jp

0-7803-9796-7/06/$20.00 ©2006 IEEE

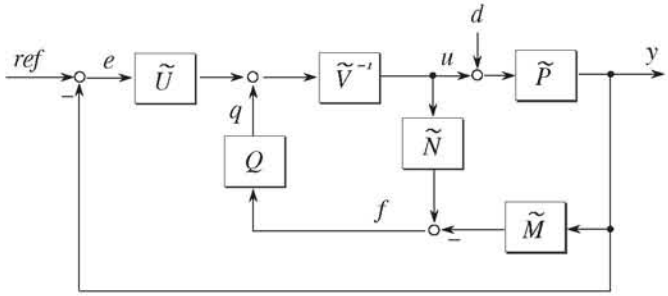

Fig. 1. GIMC structure

This residual $f(s)$ is an error of an estimated output signal and an actual output signal. Consider two cases which are $\tilde{P}(s) = P(s)$ and $\tilde{P}(s) \neq P(s)$ cases.

$\tilde{P}(s) = P(s)$:

If there are no model uncertainties, disturbance nor faults, then $f(s) = 0$ and $q(s) = 0$. The control system is controlled by the high performance controller $K_0(s) = \tilde{V}(s)^{-1}\tilde{U}(s)$.

$\tilde{P}(s) \neq P(s)$:

If there are either model uncertainties or disturbance or faults, then inner loop will be active because $q(s) \neq 0$ nor $f(s) \neq 0$. The feedback system is controlled by $K(s) = (\tilde{V}(s) - Q(s)\tilde{N}(s))^{-1}(\tilde{U}(s) + Q(s)\tilde{M}(s))$.

GIMC structure can switch two controllers $K_0(s)$ and $K(s)$ by using internal signal $f(s)$ in the above way and this switching characteristic gives a desired control property to the control system. The high performance controller $K_0(s)$ is applied to the nominal plant ($f(s) = 0$) and the high robustness controller $K(s)$ is employed for the perturbed plant($f(s) \neq 0$).

B. Design Procedure of GIMC Structure

The design procedure of GIMC structure is given by the following three steps.

Design Procedure[3]

Step 1. Design a high performance controller $K_0(s)$ for the nominal model $P(s)$.

Step 2. Design a high robust controller $K(s)$ for the perturbed model $\tilde{P}(s)$.

Step 3. Construct internal controller $Q(s)$ based on the following equation.

$$Q(s) = \tilde{V}(s)(K(s) - K_0(s))(\tilde{N}(s)K(s) + \tilde{M}(s))^{-1} \quad (5)$$

The internal controller $Q(s)$ is not used for the nominal model then the nominal plant is controlled by only $K_0(s)$. The internal controller $Q(s)$ is activated for the perturbed plant and it is controlled by $K(s)$.

C. Implementation of GIMC-based Multiple Switching Controller

Actually it is impossible to construct a completely accurate plant model such as $\tilde{P}(s) = P(s)$, then $K(s)$ is applied anytime even for the nominal plant. Consider a modified GIMC structure with a detector and a switch in the internal loop as shown in Fig.2. This structure makes the high performance controller $K_0(s)$ work even if there exists a small perturbation $\tilde{P}(s) \simeq P(s)$.

In this new structure, a switching timing and its decision is judged by a residual signal $r(s)$ which is an output of a function $H(s)$. The signal $r(s)$ is expressed in eq. (6) and the function $H(s)$ is a filter of the signal $f(s)$ to judge a switching timing of the controllers.

$$r(s) = H(s)(\tilde{N}(s)u(s) - \tilde{M}(s)y(s)) \quad (6)$$

A judgment index J_{th} is a magnitude of the signal $r(s)$ in (7). This index J_{th} is utilized to decide one model among the multiple candidates of the plant models. If $r(s) \leq J_{th}$ then switch is OFF, which means the candidate of the perturbed plant is selected and if $r(s) > J_{th}$ then the switch is ON.

$$J_{th} = \max_{\Delta=0,u,d} |r(s)|, \quad \tilde{P} = P(1+\Delta) \quad (7)$$

The switching control are executed according to the free parameter Q and this method can be extended to multiple-controller case by using multiple free parameters $Q(s)$s as shown in Fig.2. In this case, we carry out **Step 2** and **Step 3** of GIMC design steps twice, and design two robust controllers $K_1(s)$ and $K_2(s)$, then construct two internal controllers $Q_1(s)$ and $Q_2(s)$ respectively.

Here two judgment indexes J_{th1} and J_{th2} are necessary and the switching control law is described as follows.

- $r(s) < J_{th1} \rightarrow$ without $Q(s) \rightarrow K_0(s)$
- $J_{th1} \leq r(s) < J_{th2} \rightarrow Q_1(s) \rightarrow K_1(s)$
- $J_{th1} \leq r(s) \rightarrow Q_2(s) \rightarrow K_2(s)$

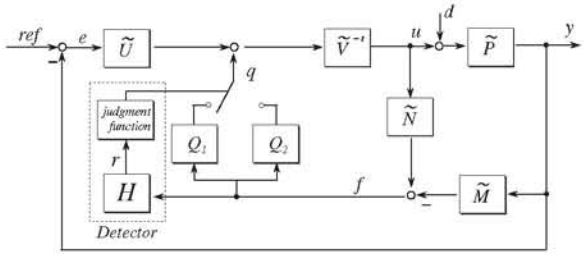

Fig. 2. Implementation of multiple controllers based on GIMC structure

III. SYSTEM CONFIGURATION AND MODELING

A. System Configuration and Modeling

We have constructed an experimental system for magnetic suspended steel plates shown in Fig.3. This system has five electromagnets and four of them are used in the feedback control where four electromagnets are identical. Each electromagnet has its own optical gap sensor across the steel plate as shown in Fig.3.

This system can be illustrated in Fig.4 where f_{magj}: electromagnetic force at each position, y_j: displacement of each position of sensor, a: distance of working point of electromagnetic force at x and z axes($j = 1,2,3,4$).

We define motion modes of the plate as in Fig.5 where y_n is a displacement of each mode of motion($n = g, \theta, \phi, \sigma$). These modes of motion are expressed in eq.(8), (9), (10) and (11). The transformation of state variable as $y_\theta = a\theta$ and $y_\phi = a\phi$ are used in these equation, where m:mass of steel plate[kg], g:acceleration of gravity[m/s^2], $M_\theta = Ix/a^2$:mass in y_θ[kg], $M_\phi = I_z/a^2$:mass in y_ϕ[kg], I_x:inertial mass of x axis[kgm^2], I_z:inertial mass of z axis[kgm^2], M_σ:mass of 4th mode[kg], C_σ:damping of 4th mode[Ns/m], K_σ:spring of 4th mode[N/m].

$$m\ddot{y}_g = mg - (f_{mag1} + f_{mag2} + f_{mag3} + f_{mag4}) \quad (8)$$

$$M_\theta \ddot{y}_\theta = -(f_{mag1} + f_{mag2} - f_{mag3} - f_{mag4}) \quad (9)$$

$$M_\phi \ddot{y}_\phi = -(f_{mag1} - f_{mag2} + f_{mag3} - f_{mag4}) \quad (10)$$

$$M_\sigma \ddot{y}_\sigma + C_\sigma \dot{y}_\sigma + K_\sigma y_\sigma = -(f_{mag1} - f_{mag2} - f_{mag3} + f_{mag4}) \quad (11)$$

The electromagnetic force is expressed in eq.(12) and it is linearized into (12) by using Taylor-series expansion, where Y_j:steady gap between electromagnet and steel plate[m], y_j:displacement from the steady gap[m], I_j:steady current of the electromagnet[A], i_j:current from steady current[A], and k and y_{0j} are coefficients of electromagnets.

$$f_{magj}(t) = k_j \left(\frac{I_j + i_j(t)}{Y_j + y_j(t) + y_{0j}} \right)^2 \quad j = 1,2,3,4$$
$$\simeq K_{eq} + K_i i_j(t) - K_y y_j(t) \quad (12)$$
$$K_{eq} = k\left(\frac{I}{Y+y_0}\right)^2, \; K_i = \frac{2kI}{(Y+y_0)^2}, \; K_y = \frac{2kI^2}{Y+y_0)^3}$$

Let us define the coordinate translation matrix T between each axis($j = 1,2,3,4$) and each mode of motion($n = g, \theta, \phi, \sigma$) as

$$\begin{bmatrix} y_1 \\ y_2 \\ y_3 \\ y_4 \end{bmatrix} = T \begin{bmatrix} y_g \\ y_\theta \\ y_\phi \\ y_\sigma \end{bmatrix}, \; T = \begin{bmatrix} 1 & 1 & 1 & 1 \\ 1 & 1 & -1 & -1 \\ 1 & -1 & 1 & -1 \\ 1 & -1 & -1 & 1 \end{bmatrix} \quad (13)$$

Substitute eq.(12) into (8), (9), (10) and (11) with a relation of $mg = 4K_{eq}$ at the equilibrium point, then we can obtain the equations of motion of each mode as in (14), (15), (16) and (17) by using the matrix T.

$$\ddot{y}_g(t) = \frac{4K_y}{m} y_g(t) - \frac{4K_i}{m} i_g(t) \quad (14)$$

$$\ddot{y}_\theta(t) = \frac{4K_y}{M_\theta} y_\theta(t) - \frac{4K_i}{M_\theta} i_\theta(t) \quad (15)$$

$$\ddot{y}_\phi(t) = \frac{4K_y}{M_\phi} y_\phi(t) - \frac{4K_i}{M_\phi} i_\phi(t) \quad (16)$$

$$\ddot{y}_\sigma(t) = -\frac{C_\sigma}{M_\sigma}\dot{y}_\sigma + \left(\frac{4K_i - K_\sigma}{M_\sigma}\right) y_\sigma - \frac{4K_i}{M_\sigma} i_\sigma \quad (17)$$

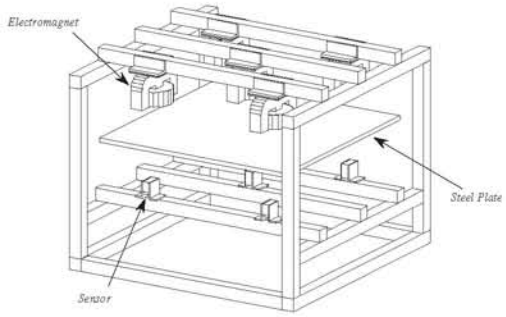

Fig. 3. Magnetically Suspended Steel Plate System

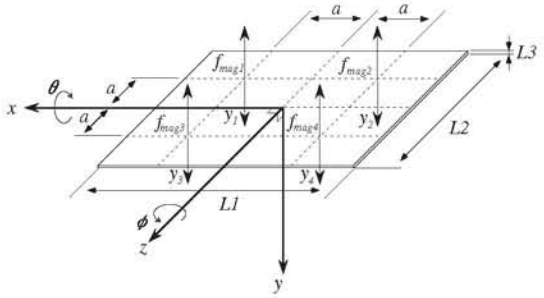

Fig. 4. Axes and forces to the Plate

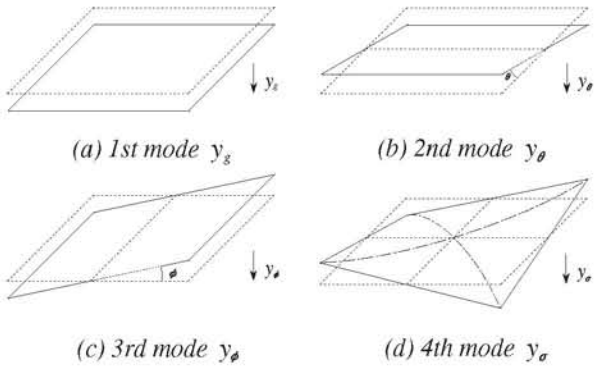

(a) 1st mode y_g (b) 2nd mode y_θ

(c) 3rd mode y_ϕ (d) 4th mode y_σ

Fig. 5. Motion Modes of the Plate

B. Definition of Multiple Plants

Let us define multiple plants shown in Fig.6. The **nominal suspended object** is constructed with a steel plate with two aluminum plates on it and its corresponding mathematical model is defined as $P(s)$. The **perturbed object 1** is also constructed with a steel plate with one aluminum plate on it and its mathematical model is defined as $\tilde{P}_1(s)$ and **perturbed object 2** is a steel plate itself and its mathematical model is defined as $\tilde{P}_2(s)$. A mass of a steel plate is 1.877[kg] and a mass of an aluminum plate is 0.333[kg]. The physical parameters for $P(s)$, $\tilde{P}_1(s)$ and $\tilde{P}_2(s)$ are also shown in Table I.

IV. CONTROL SYSTEM DESIGN

The controller is designed for each mode($n = g, \theta, \phi, \sigma$) based on the design procedure described above. First, a nominal high performance controller $K_0(s)$ for $P(s)$ is designed in **Step1**, then the robust controllers $K_1(s)$ and $K_2(s)$ for $\tilde{P}_1(s)$, $\tilde{P}_2(s)$ are also designed in **Step2.1** and **2.2**, respectively. $\mathscr{H}_\infty$

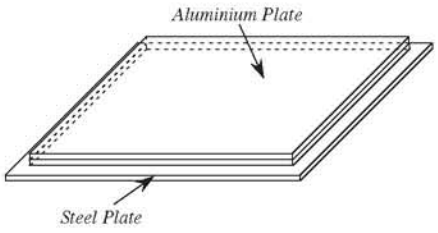

Fig. 6. Nominal Suspended Object

TABLE I
MODEL PARAMETERS

	$P(s)$	$\tilde{P}_1(s)$	$\tilde{P}_2(s)$
m[kg]	2.543	2.210	1.877
I_x[kgm^2]	5.087×10^{-2}	4.512×10^{-2}	3.937×10^{-2}
I_z[kgm^2]	5.087×10^{-2}	4.512×10^{-2}	3.937×10^{-2}
Y[m]	5×10^{-3}		
I[A]	0.431	0.402	0.370
k[Nm^2/A^2]	12.340×10^{-4}		
y_0[m]	1.044×10^{-3}		
M_σ[kg]	6.511[kg]	5.775[kg]	5.040[kg]
C_σ[Ns/m]	10		
K_σ[N/m]	5×10^4		

mixed sensitivity problem is used for the controller design. The designed controllers K_0 is shown in Fig.7, K_1 and K_2 are omitted. From these three figures, we can see that the gain curves of K_0, K_1 and K_2 are on the decrease in this order. Therefore, performance of K_0, K_1 and K_2 are better in that order. On the other hand, robustness of K_2, K_1 and K_0 are on the increase.

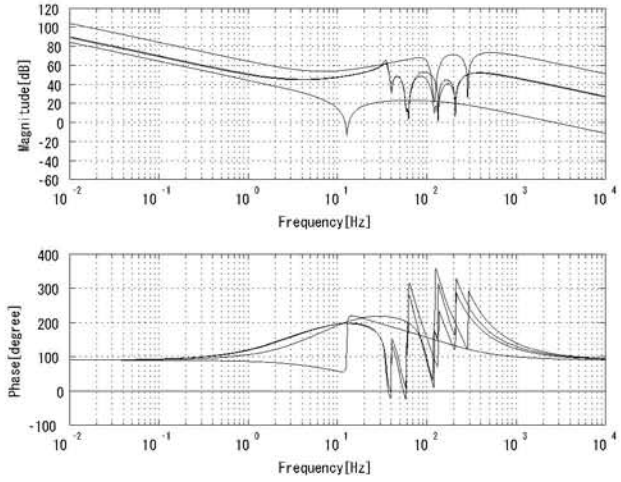

Fig. 7. Bode Diagram of Controller K_0

Finally, we construct the internal controller $Q_1(s)$ and $Q_2(s)$ by using $K_0(s)$, $K_1(s)$ and $K_2(s)$ based on **Step 3**. In order to construct the internal controller in (5), the coprime factorizations of $P(s)$ and $K_0(s)$ are required. Suppose that state space representations of $K_0(s)$ and $P(s)$ are given as

$$P = \left[\begin{array}{c|c} A & B \\ \hline C & D \end{array}\right], \quad K_0 = \left[\begin{array}{c|c} A_k & B_k \\ \hline C_k & D_k \end{array}\right] \tag{18}$$

where (A,B) and (A_k,B_k) are controllable, (C,A) and (C_k,A_k) are observable. The coprime factorizations of $P(s)$ and $K_0(s)$ are given by (19) and (20), respectively. Note that L and L_k stabilize $A+LC$ and $A_k+L_kC_k$, respectively.

$$\left[\begin{array}{cc} \tilde{N} & \tilde{M} \end{array}\right] = \left[\begin{array}{c|cc} A+LC & B+LD & L \\ \hline C & D & I \end{array}\right] \tag{19}$$

$$\left[\begin{array}{cc} \tilde{V} & \tilde{U} \end{array}\right] = \left[\begin{array}{c|cc} A_k+L_kC_k & L_k & B_k+L_kD_k \\ \hline C_k & I & D_k \end{array}\right] \tag{20}$$

For comparison, we designed a μ-synthesis controller and the bode plot of the controller K_μ is shown in Fig.8. The gain characteristic of K_μ is similar to a gain curve of K_2. The structured singular value μ with the K_μ is less than one. Therefore, K_μ achieves the robust performance condition.

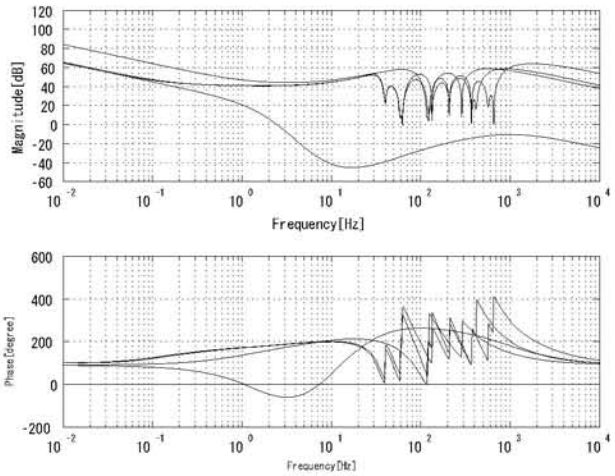

Fig. 8. Bode Diagram of Controller K_μ

V. EXPERIMENTAL EVALUATION

A. Evaluation of performance and robustness

Impulse disturbance responses are shown in Fig.9 and Fig.10. The magnitude of the disturbance is about 12[N] upward impulse force from under the steel plate. From the result of disturbance responses, GIMC structure shows worse response in (c)-case but shows better responses in (a) and (b)-cases. The μ-controller K_μ does not show big change in all cases. However, a response of K_μ in Fig.10(c) is vibrating in a steady state which means this condition is almost robust stability limit. GIMC in Fig.9(c) does not show any vibration in a steady state after 1[s] which shows robustness of the GIMC structure. A response of GIMC in Fig.9(a) shows better response than K_μ which means GIMC has a better nominal performance. From these results, K_μ achieves performance and robustness, but can't achieve high performance in nominal case and high robustness in the perturbed case. On the other hand, GIMC structure achieves both of high performance in nominal case and high robustness in perturbed case.

B. Evaluation of controller switching

We remove one aluminum plate from the nominal plant at 10[s] and remove another aluminum plate at 30[s]. The resulting time responses in the change of the suspended plates are shown in Fig.11. The response of GIMC structure does not change in steady state, but the response of K_μ change and its vibration is getting larger after 30[s] for $\tilde{P}_2$. The GIMC structure changes the magnitude of the control input by controller switching according to the plant variation, but the magnitude of the control input of K_μ is almost invariant for all three plants. The internal signal r which is an output of the filter $H(s)$ in these situations is shown in Fig.12. It can be seen that GIMC structure can detect a perturbation of plant by using this internal signal. In this case, threshold values of judgment functions are selected as $J_{th1} = 0.7 \times 10^{-4}$ and $J_{th2} = 2.5 \times 10^{-4}$.

VI. CONCLUSION

This paper dealt with an application of GIMC-based switching control to a magnetically suspended steel plate system. We considered the multiple suspended objects and verify that GIMC structure achieved both of high performance for the nominal plant and high robustness for the perturbed plants by controller switching. We designed three robust controllers and they were appropriately switched in the GIMC structure according to the internal residual signal. A robust single controller which achieved the robust performance condition based on the structured singular value μ was designed for comparison. We showed that the conventional μ-controller had the robust performance but the nominal performance was sacrificed for robustness. On the other hand, the proposed GIMC controller had better nominal performance compared with the μ controller, and also achieved higher robust stability for multiple plants.

REFERENCES

[1] Kemin Zhou and John C.Doyle, *Essential of Robust Control*, Prentice Hall, 1998

[2] Gier E.Dullerud and Fernando Paganini, *A Course in Robust Control Theory : A Convex Approach*, Springer, 1999

[3] Kemin Zhou, A Natural Approach to High Performance Robust Control: Another Look at Youla Parameterization, *Proceedings of SICE Annual Conference 2004*, pp.869-874, 2004

[4] Kemin Zhou and Zhang Ren, A New Controller Architecture for High Performance, Robust , and Fault-Tolerant Control, *IEEE Transaction on Automatic Control*, Vol.46, No.10, pp.1613-1618, 2001

[5] Daniel U,Campos-Delgado and Kemin Zhou, Reconfigurable Fault-Tolerant Control Using GIMC Structure, *IEEE Transactions on Automatic Control*, Vol.48, No.5, pp.1613-1618, 2003

[6] D.U.Campos-Delgado, S.Martinez Martinez and K.Zhou, Integrated Fault Tolerant Scheme with Disturbance Feedforward, *Proceeding of the 2004 American Control Conference*, pp.1799-1804, 2004

[7] Henrik Niemann, Jakob Stoustrup, Passive fault tolerant control of a double inverted pendulum - a case study, *Control Engineering Practice, vol. 13, pp.1047-1059, 2005*

[8] Mimpei Morishita and Tsukasa Ide, Constant Gap Width Control for Magnetic Levitation System by Attracting Force, T. IEE Japan, Vol.103-B, No.6, pp.403-409, 1983(in Japanese)

[9] Toru Namerikawa and Daisuke Mizutani , Robust H_∞ DIA Control of Levitated Steel Plates ,Proc. of the Fifth International Symposium on Liner Drives for Industry Applications(LDIA2005), pp.310-313, 2005

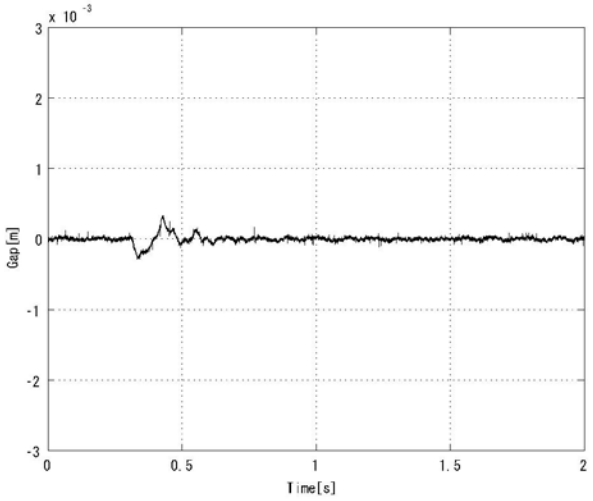

(a) $P(s)$

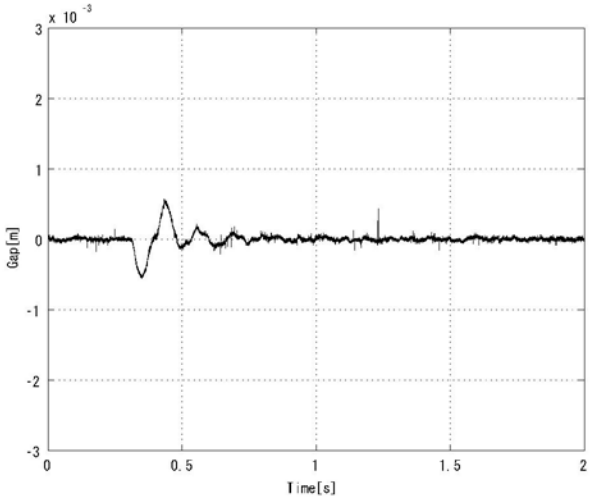

(b) $\tilde{P}_1(s)$

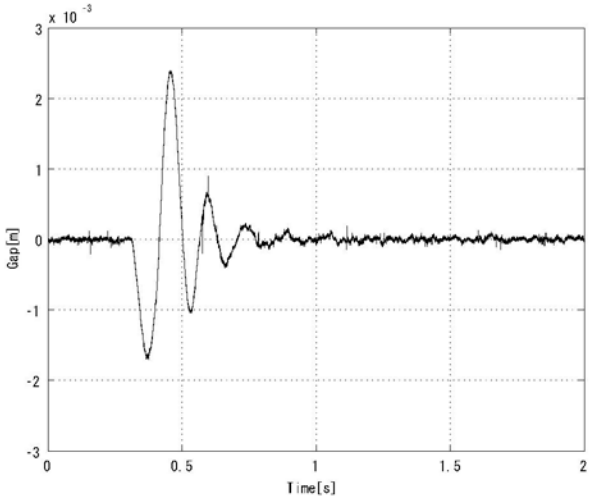

(c) $\tilde{P}_2(s)$

Fig. 9. Disturbance Response of GIMC

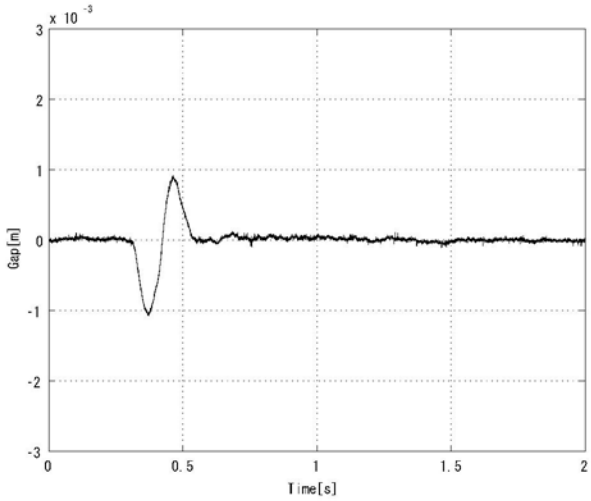

(a) $P(s)$

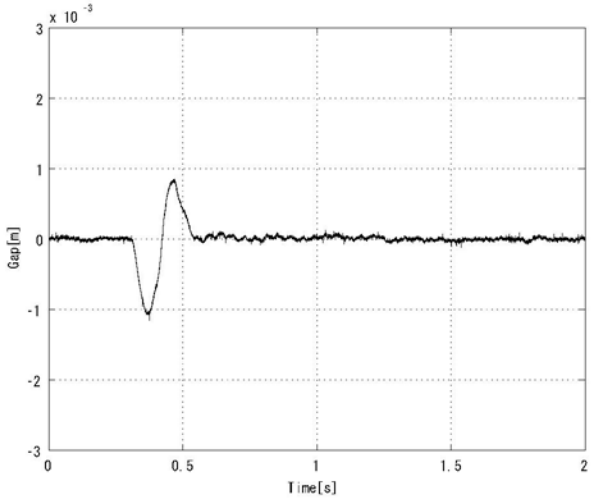

(b) $\tilde{P}_1(s)$

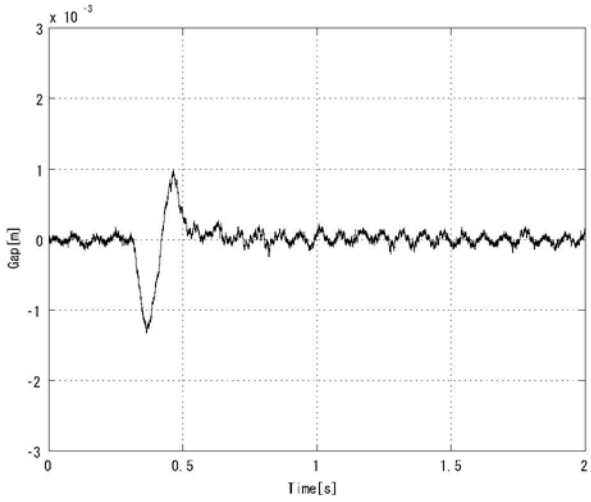

(c) $\tilde{P}_2(s)$

Fig. 10. Disturbance Response of K_μ

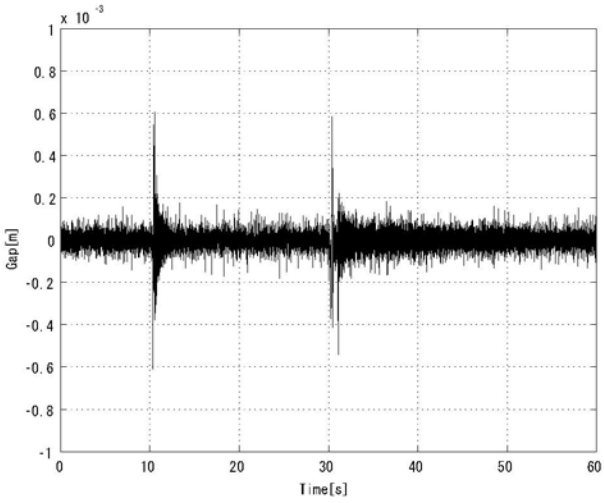

(a) GIMC

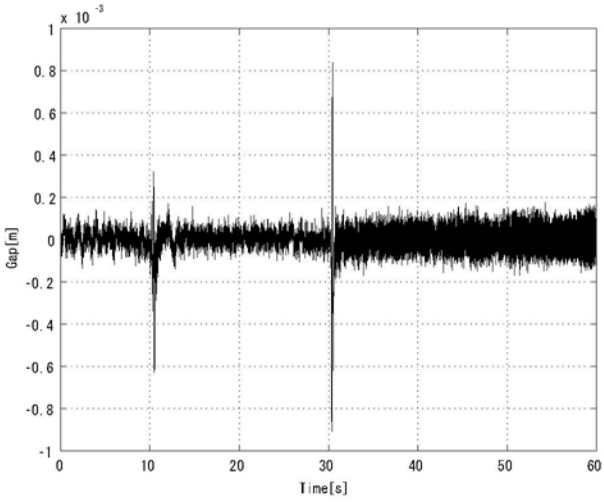

(b) K_μ

Fig. 11. Time Responses with Model Change: $P \rightarrow \tilde{P}_1 \rightarrow \tilde{P}_2$

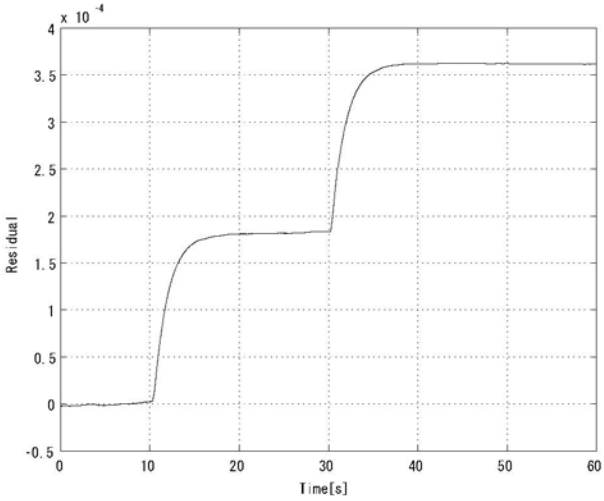

Residual Signal $r(t)$

Fig. 12. Time Responses of $r(t)$ with Model Change: $P \rightarrow \tilde{P}_1 \rightarrow \tilde{P}_2$